



TAMPERE UNIVERSITY OF TECHNOLOGY

**Mikko Poikkimäki**  
**SOA formation yields in chamber**

Updated: 16.8.2013

# TABLE OF CONTENTS

1. Introduction . . . . .	1
2. Theory . . . . .	2
2.1 Diffusion in binary mixtures . . . . .	2
2.1.1 Alternative . . . . .	3
2.2 Condensation sink . . . . .	5
2.3 Proposed chemical reaction of monoterpene, SLLV source . . . . .	6
3. Methods . . . . .	7
3.1 Used sectional model . . . . .	7
3.2 How model was used . . . . .	8
3.3 Analysing tools for results, how to get $\alpha$ and $\gamma$ ? . . . .	9
4. Results . . . . .	11
4.1 Results using $\text{H}_2\text{SO}_4$ values . . . . .	11
4.2 Results using $\text{C}_{10}\text{H}_{16}\text{O}_{10}$ values . . . . .	15
4.2.1 Mass- $\alpha$ figures . . . . .	19
5. Matlab scripts and data files . . . . .	22
6. Conclusion . . . . .	23
6.1 What next? . . . . .	23
References . . . . .	24

## **1. INTRODUCTION**

## 2. THEORY

### 2.1 Diffusion in binary mixtures

Diffusion illustrates mass convection in medium from greater concentration to lower concentration. Fick's law states diffusion flux

$$J = -D_{AB} \frac{dn}{dx}, \quad (2.1)$$

where  $D_{AB}$  is binary diffusion coefficient and  $n$  molecule number concentration.

Diffusion coefficient for binary gasmixtures can be calculated from Reid et al. (1987)

$$D_{AB} = 0.001 \cdot T^{1.75} \frac{\sqrt{\frac{1}{M_A} + \frac{1}{M_B}}}{p(V_A^{1/3} + V_B^{1/3})^2}, \quad (2.2)$$

where unit of diffusion coefficient is  $\text{cm}^2/\text{s}$ , temperature  $T$  is Kelvin, molar masses  $M$  are  $\text{g/mol}$  and pressure  $p$  is bar. Diffusion volumes  $V$  can be calculated from values for atomic diffusion volumes which are for carbon C 15.9, for hydrogen 2.31, for oxygen 6.11, for nitrogen 4.54, for heterocyclic ring -18.3 and for air 19.7.

Diffusion related vapor mean free path according to Pirjola and Kulmala (1998)

$$\lambda = \frac{3D_{AB}}{\bar{c}_A}, \quad (2.3)$$

where  $\bar{c}_A$  is velocity of gas molecules

$$\bar{c}_A = \sqrt{\frac{8RT}{\pi M_A}}, \quad (2.4)$$

where  $R$  is ideal gas constant  $8.31446 \text{ J/Kmol}$ .

For example  $\text{C}_{10}\text{H}_{16}\text{O}_{10}$  molecule ( $M_A \approx 300$ ) with one heterocyclic ring, diffusion volume  $V_A \approx 250$ . Diffusion coefficient of this molecule in air in temperature 290 K and pressure 1 atm is  $0.0489 \text{ cm}^2/\text{s}$ . Related mean free path  $\lambda$  is 102.65 nm. Few more examples are presented in figure 2.1.

Vapors in figure 2.1 are proposed to form SOA (Ehn et al. 2013).

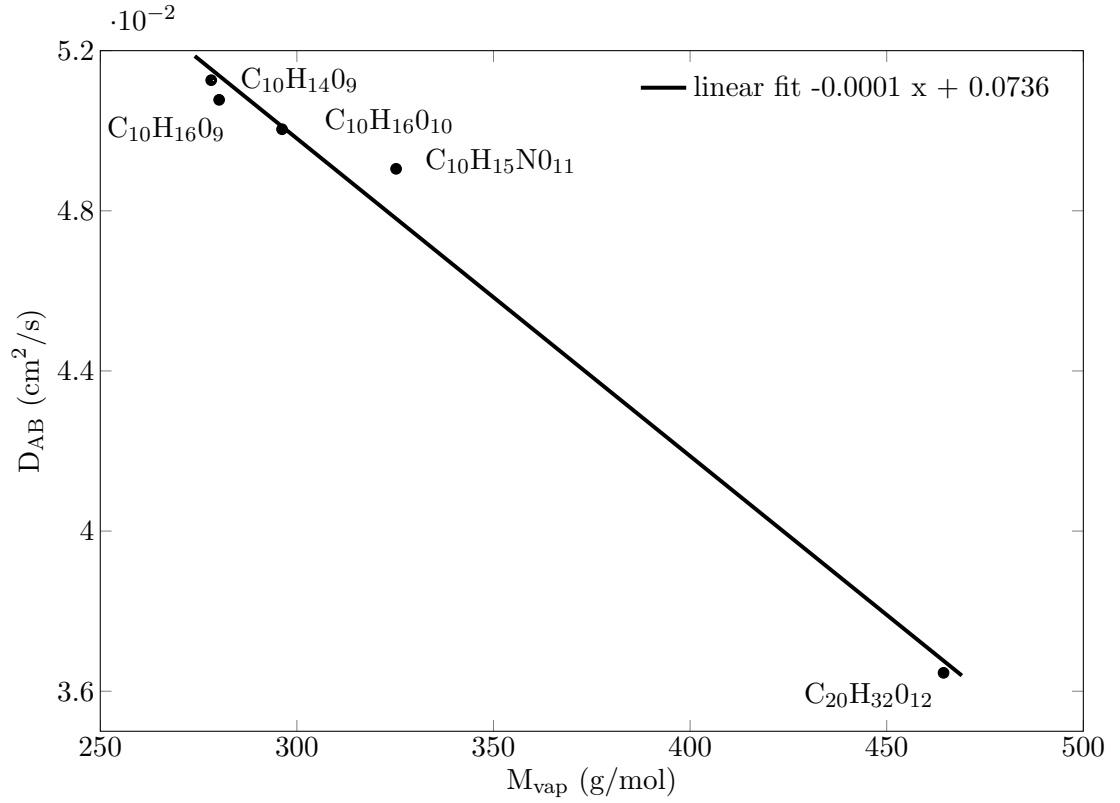


**Figure 2.1:** Binary diffusion coefficients as function of molar mass for different organic vapors calculated from equation 2.2.

### 2.1.1 Alternative

Mäkelä, J. kalvot

vapor(A) and air (B) have dilute mixture. For this two gases binary mixture we have to determine free path  $\lambda$  and diffusion coefficient  $D$  for both components.

vapormolecule diffusion coefficient in the air

$$D_{AB} = \frac{3}{8\pi} \frac{[\pi k_B^3 T^3 (1 + z_{AB}) / (2m_A)]^{1/2}}{\rho \sigma_{AB}^2 \Omega_{AB}^{(1,1)}}, \quad (2.5)$$

and related vapor molecule free path

$$\lambda_{AB} = \frac{32}{3\pi(1 + z_{AB})} \frac{D_{AB}}{\bar{c}_A}, \quad (2.6)$$

before it collides next time to air molecule.

Average collision area

$$\sigma_{AB} = \frac{\sigma_A + \sigma_B}{2}, \quad (2.7)$$

Ratio of molemasses

$$z_{AB} = \frac{M_A}{M_B}, \quad (2.8)$$

collision integral  $\Omega_{AB}^{(1,1)} = 1$  for hard spheres

Chapman-Enskog 1939 for more info

Chapman, Sydney, and Thomas George Cowling. The mathematical theory of non-uniform gases: an account of the kinetic theory of viscosity, thermal conduction and diffusion in gases. Cambridge university press, 1970.

S. Chapman and T. G. Cowling, The Mathematical Theory of Nonuniform Gases (Cambridge University Press, Cambridge, 1952).

Marrero, T.R. and Mason E.A. 1972 comment to Chapman-Enskog on page 8 section 2.2b

Mass

$$m = \rho V \Rightarrow V = \frac{m}{\rho}, \quad (2.9)$$

Otherwise

$$m = nM = \frac{N}{N_A}M, \quad (2.10)$$

Now considering one molecule ( $N=1$ )

$$m = nM = \frac{M}{N_A}, \quad (2.11)$$

Considering molecule as sphere, volume

$$V = \frac{\pi}{6}d_p^3 \Rightarrow d_p = \sqrt[3]{\frac{6V}{\pi}}, \quad (2.12)$$

Equation 2.11 to equation 2.9

$$V = \frac{M}{\rho N_A}, \quad (2.13)$$

Then equation 2.13 to equation 2.12, diameter of spherical molecule

$$d_p = \sqrt[3]{\frac{6M}{\pi \rho N_A}}, \quad (2.14)$$

Example for molecule which mass = 300 g/mol and density  $\rho = 1.1 \text{ g/cm}^3$

$$d_p = \sqrt[3]{\frac{6 \cdot 300 \cdot 10^{-3} \text{ kg/mol}}{\pi \cdot 1100 \text{ kg/m}^3 \cdot 6.022 \cdot 10^{23} \text{ 1/mol}}} \approx 0.95 \text{ nm}, \quad (2.15)$$

Example for sulfuric acid  $\text{H}_2\text{SO}_4$  molecule which mass = 98.08 g/mol and density  $\rho = 1.84 \text{ g/cm}^3$

$$d_p = \sqrt[3]{\frac{6 \cdot 98.08 \cdot 10^{-3} \text{ kg/mol}}{\pi \cdot 1840 \text{ kg/m}^3 \cdot 6.022 \cdot 10^{23} \text{ 1/mol}}} \approx 0.553 \text{ nm}, \quad (2.16)$$

Example for airmolecule which mass = 29 g/mol and density

$$\rho = \frac{Mp}{RT} = \frac{29 \cdot 10^{-3} \text{ kg/mol} \cdot 101300 \text{ Pa}}{8.31446 \text{ JK}^{-1} \text{ mol}^{-1} \cdot 290 \text{ K}} = 1.22 \text{ g/cm}^3 \quad (2.17)$$

$$d_p = \sqrt[3]{\frac{6 \cdot 29 \cdot 10^{-3} \text{ kg/mol}}{\pi \cdot 1220 \text{ kg/m}^3 \cdot 6.022 \cdot 10^{23} \text{ 1/mol}}} \approx 0.42 \text{ nm}, \quad (2.18)$$

according to Mäkelä, J.  $d_{p_{air}} = 0.37 \text{ nm}$

Wikipedia S. Chapman, T. G. Cowling (1970) The Mathematical Theory of Non-uniform Gases: An Account of the Kinetic Theory of Viscosity, Thermal Conduction and Diffusion in Gases, Cambridge University Press (3rd edition), ISBN 052140844X.  
for rigid spheres

$$D_{AB} = \frac{3}{8n(d_1 + d_2)^2} \left[ \frac{k_B T (m_1 + m_2)}{2\pi m_1 m_2} \right]^{1/2}, \quad (2.19)$$

## 2.2 Condensation sink

Condensation sink represents rate how rapidly condensable vapor molecules condenses on existing aerosol in units 1/s. It can be calculated from

$$CS = 2\pi D \int_0^\infty d_p \beta(d_p) n(d_p) dd_p = 2\pi D \sum_i \beta d_{pi} N_i, \quad (2.20)$$

where  $d_{pi}$  is the diameter of a particle in size class  $i$ ,  $N_i$  is corresponding particle number concentration (Dal Maso et al., 2002) and  $D$  is diffusion coefficient of condensing vapor. Transition regime correction factor  $\beta_m$  according to Fuchs and Sutugin (1971) is

$$\beta_m = \frac{1 + Kn}{1 + \left( \frac{4}{3\alpha_m} + 0.337 \right) Kn + \frac{4}{3\alpha_m} Kn^2} \quad (2.21)$$

where  $\alpha_m$  is the sticking coefficient which represents probability of molecule to

stick in to the particle. Dimensionless Knudsen number is

$$Kn = \frac{2\lambda}{d_p}, \quad (2.22)$$

where  $\lambda$  is the effective mean free path of the condensing vapor molecules in the gas. Knudsen number is the ratio of two length scales. Mean free path  $\lambda$  characterizes the gas with respect to the transport of mass and particle diameter  $d_p$  characterizes the droplet.

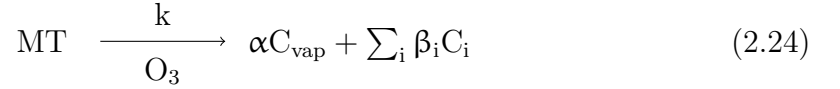
One can semiempirically represent condensation sink as a function of aerosol mass as follows

$$CS = 2 \cdot 10^{-4} \cdot N^{0.37} M^{0.63}, \quad (2.23)$$

where  $N$  is particle number and  $M$  particle mass.

### 2.3 Proposed chemical reaction of monoterpene, SLLV source

Monoterpene reaction with ozone produces SLLV product with mass yield of  $\alpha$  and other products with mass yields of  $\beta_i$



Source of SLLV vapor is then

$$Q = \alpha k P, \quad (2.25)$$

where  $P = P_0 e^{-kt}$  is precursor (monoterpene) concentration and overall reaction rate  $k = k'[O_3]$  is reaction rate of ozone times ozone concentration.

Proposed SLLV product sinks

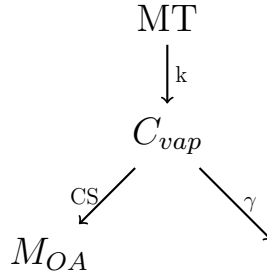


**Figure 2.2:** Proposed routes for monoterpene precursor MT reaction (rate  $k$ ) SLLV product  $C_{\text{vap}}$ . To aerosol  $M_{OA}$  with rate  $CS$  or to walls or other losses with rate  $\gamma$



### 3. METHODS

Particle size distribution varies in time through different processes as nucleation, condensation, coagulation, sedimentation and dilution. These changes can be modelled with general dynamic equation (GDE) (Seinfeld and Pandis, 1998)

$$\begin{aligned} \frac{\partial n(v, t)}{\partial t} = & \frac{1}{2} \int_0^v K(v-q, q) n(v-q, t) dq - n(v, t) \int_0^\infty K(q, v) n(q, t) dq \\ & - \frac{\partial}{\partial v} [I(v) n(v, t)] + J_0 \delta(v - v_0) + S(v) - R(v), \end{aligned} \quad (3.1)$$

where  $I$  is particle volume changing rate,  $J_0$  is nucleation rate,  $K$  is coagulation coefficient,  $n$  is size distribution function,  $R$  particle loss rate,  $S$  particle sources emission rate,  $t$  is time,  $v$  and  $q = v + dv$  are particle volumes and  $\delta(v - v_0)$  is Dirac's delta function which is one whenever  $v = v_0$  and otherwise zero. Two first term of equation represents coagulation, third term condensation, fourth nucleation, fifth other particle sources and the last other particle sinks like deposition.

#### 3.1 Used sectional model

In sectional model particle size distribution is divided in desired amount of size sections which are characterized with two parametres: particle size and concentration. Particle population is considered monodispersive in each section. In this study moving center model was used where section borders are fixed but particle sizes can vary inside sections (Korhonen, 2004). Model takes into account particle coagulation and dilution, vapor condensation in to the particles, vapor dilution and loss to walls (or other places).

Coagulation is modelled with parts of discrete general dynamic equation (Seinfeld and Pandis, 1998)

$$\frac{dN_k}{dt} = \frac{1}{2} \sum_{j=g^*}^{k-g^*} K_{j,k-j} N_j N_{k-j} - N_k \sum_{j=g^*}^{\infty} K_{k,j} N_j, \quad (3.2)$$

where first term represents increase of particles in section  $k$  and second term reduction of particles through coagulation.

Condensation growth of particles is modelled by growing section size using growth

rate (Seinfeld and Pandis, 1998)

$$\frac{dd_p}{dt} = \frac{2M_{vap}I}{\pi\rho d_p^2 N_A}, \quad (3.3)$$

where  $M_{vap}$  is condensing vapor molecular mass,  $\rho$  particle density,  $N_A$  Avogadro's number and  $I$  flux of molecules to the particle phase. It is obtained from

$$I = 2\pi d_p D C_{vap} \beta_m, \quad (3.4)$$

where  $D$  is diffusion coefficient,  $C_{vap}$  concentration of condensing vapor and  $\beta_m$  obtained from equation 2.21.

Dilution of particle concentration is modelled with equation

$$\frac{dN_k}{dt} = -\gamma_{dil} N_k, \quad (3.5)$$

where  $\gamma_{dil}$  is dilution coefficient in units 1/s. It is inverse value of aerosol lifetime  $\tau$ .

Used condensing vapor concentration gradient

$$\frac{dC_{vap}}{dt} = Q - CS \cdot C_{vap} - \gamma C_{vap} - \gamma_{dil} C_{vap}, \quad (3.6)$$

takes into account vapor source rate  $Q$ , vapor loss rate to particles  $CS$  and to walls  $\gamma$  and vapor dilution rate  $\gamma_{dil}$ .

See connection with  $CS$  and  $I$

$$CS = \sum_i I_i N_i. \quad (3.7)$$

This is connection between particle growth and vapor loss to particles. These differential equations 3.2, 3.3, 3.5 and 3.6 are solved numerically using Runge-Kutta-method (Dormand and Prince, 1980) and time evolution of number distribution function  $dN/dd_p$  gained among other results.

### 3.2 How model was used

In this study batch type aerosol chamber was modelled with 60 size sections between sizes 1 nm and 1  $\mu$ m. Different aerosol mass seeds  $M_0$  and monoterpene concentrations  $P_0$  was used for two particle sizes and two SLLV wall loss coefficient resulting  $4 \times 4 \times 2 \times 2 = 64$  model runs. Used constants and variables are presented in table 3.1.

Aerosol total numbers for model presented in table 3.1 are calculated from aerosol

**Table 3.1:** Used values in modelling. Those values kept same in each model run are presented first and then values that changed between are under.

Constant	Symbol	Unit	Value
Stoichiometric yield of SLLV	$\alpha$	-	0.3
Sticking coefficient	$\alpha_m$	-	1
Dilution coefficient	$\gamma_{dil}$	1/s	$5 \cdot 10^{-5}$
SLLV vapor mean free path	$\lambda$	nm	102.65
Particle density	$\rho$	g/cm <sup>3</sup>	1.4
Geometric mean deviation GMD	$\sigma$	-	1.3
Diffusion coefficient of SLLV	$D_{AB}$	cm <sup>2</sup> /s	0.0489
Reaction rate of ozone	$k'$	1/s	$2 \cdot 10^{-16}$
Molar mass of SLLV	$M_{vap}$	g/mol	300
Molar mass of monoterpene	$M_{MT}$	g/mol	137
Ozone concentration	$[O_3]$	ppb	60
Pressure	$p$	atm	1
Temperature	$T$	K	290
Time vector	$t$	s	0 - 36000
Variable	Symbol	Unit	Value
SLLV wall loss coefficient	$\gamma$	1/s	0.02, 0.002
Count median diameter CMD	$\mu$	nm	10, 80
Aerosol mass seed (10 nm particles)	$M_{10nm}$	ng/m <sup>3</sup>	3, 15, 30, 100
Related number (10 nm particles)	$N_{10nm}$	10 <sup>3</sup> 1/cm <sup>3</sup>	$\sim 4, 20, 41, 137$
Aerosol mass seed (80 nm particles)	$M_{80nm}$	μg/m <sup>3</sup>	1, 5, 10, 30
Related number (80 nm particles)	$N_{80nm}$	10 <sup>3</sup> 1/cm <sup>3</sup>	$\sim 2.7, 13, 27, 80$
Initial monoterpene concentration	$P_0$	ppb	10, 50, 100, 200

mass seed using count median diameter as size of particles

$$N = \frac{m}{\rho(\pi/6)\mu^3}. \quad (3.8)$$

Then lognormal distribution is produced with CMD, GMD and N.

Conversion of ppb to 1/cm<sup>3</sup> is done multiplying with  $p/kT = 2.5331 \cdot 10^{19}$  air molecules/cm<sup>3</sup>.

### 3.3 Analysing tools for results, how to get $\alpha$ and $\gamma$ ?

Aerosol mass yield

$$Y = \frac{\Delta M}{\Delta P}, \quad (3.9)$$

where  $\Delta M$  is formed aerosol mass and  $\Delta P$  is used precursor mass. Formed aerosol mass can be calculated

$$\Delta M = M_{tot} - M_0 + M_{dil}, \quad (3.10)$$

where  $M_{tot}$  is aerosol total mass,  $M_0$  initial aerosol mass and  $M_{dil}$  diluted aerosol mass. From particle number distribution  $dN/dd_p$ , total aerosol number  $N_{tot}$ , volume  $V_{tot}$  and mass  $M_{tot}$  is integrated considering spherical particles with density  $\rho = 1.4 \text{ g/cm}^3$ . Diluted aerosol number  $N_{dil}$  is calculated by model from differential equation 3.5. From  $N_{dil}$  diluted mass  $M_{dil}$  can be calculated and formed aerosol mass got.

Used precursor  $\Delta P$  is calculated from

$$\Delta P = \int_0^{t_{end}} kP \, dt, \quad (3.11)$$

where  $t_{end}$  is elapsed time,  $k$  is formation rate and  $P$  is precursor concentration presented in equation 2.25.

Condensation sink was calculated from equation 2.20 using particle number distribution  $dN/dd_p$  and values of table 3.1.

Proposed relation for yield and condensation sink

$$Y_{end} = \frac{\alpha}{1 + \frac{\gamma}{CS_{end}}}. \quad (3.12)$$

Using equation 2.23, this relation can be presented as function of aerosol mass

$$Y_{end} = \frac{\alpha}{1 + \frac{\gamma}{2 \cdot 10^{-4} \cdot N^{0.37} M^{0.63}}}. \quad (3.13)$$

Fitting these functions to yield data results knowledge of stoichiometric coefficient of SLLV product  $\alpha$  and chamber wall losses  $\gamma$ .

## 4. RESULTS

### 4.1 Results using $\text{H}_2\text{SO}_4$ values

To get an idea how condensation sink and secondary organic aerosol mass varies throughout modelling time, in figures 4.1 and 4.2 are presented four examples of condensation sink and aerosol mass with different initial conditions in batch chamber. All other condensation sinks and aerosol masses of 60 cases are between or near of those lines in figures 4.1 and 4.2.

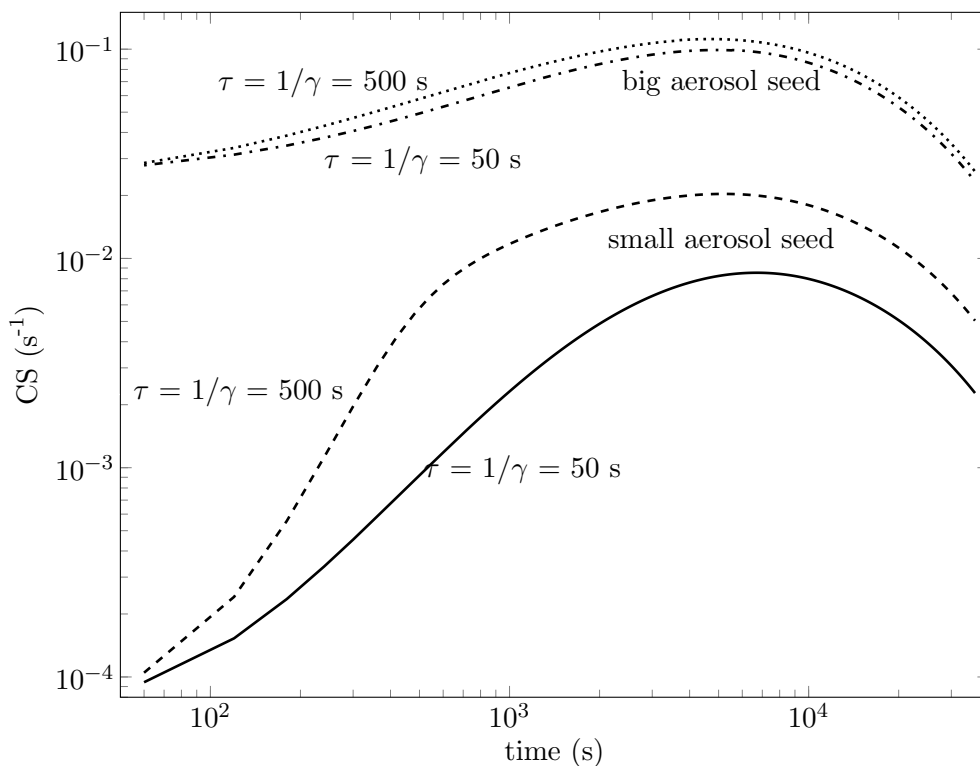


**Figure 4.1:** Condensation sink as function of modelling time in four different cases. Two lines for small ( $D_p = 10$  nm,  $M_{OA} = 3$  ngm $^{-3}$ ) and two lines for big ( $D_p = 80$  nm,  $M_{OA} = 10$   $\mu$ gm $^{-3}$ ) secondary organic aerosol mass seeds are presented with two different SLLV product lifetimes  $\tau$ .

Both condensation sink and aerosol mass grow until dilution loss is bigger than gain from aerosol growth. That happens near  $10^4$  seconds which is about 3 hours and near the times when aerosol mass yield values are stabilized, see figure 4.3.

Exactly: Yield  $Y$  and condensation sink  $CS$  values was chosen at times 6960 s

for 80 nm particles and 11280 s for 10 nm particles and final values for yield  $Y_{end}$  and condensation sink  $CS_{end}$  got.

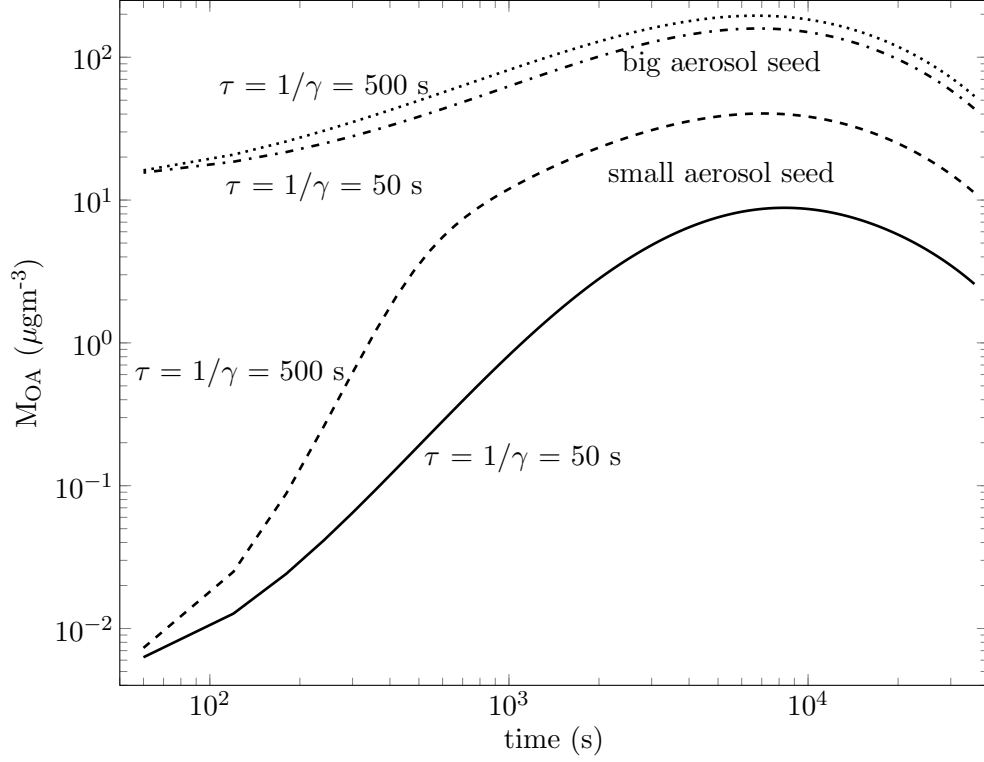


**Figure 4.2:** Secondary organic aerosol mass as function of modelling time in four different cases. Two lines for small ( $D_p = 10$  nm,  $M_{OA} = 3$  ngm $^{-3}$ ) and two lines for big ( $D_p = 80$  nm,  $M_{OA} = 10$  μgm $^{-3}$ ) secondary organic aerosol mass seeds are presented with two different SLLV product lifetimes  $\tau$ .

In figure 4.4 are aerosol mass yield values at time when they have reached constant value, see figure 4.3, as function of aerosol condensation sink. Times needed to stabilise yields are in this modelling from two to three hours. That time is considered as end time  $t_{end}$ .

One can see, comparing data points with different SLLV lifetimes in figure 4.4, that aerosol mass yields are lower when lifetime is shorter. With short vapor lifetime, there is not enough time for aerosol to grow bigger sizes (bigger CS). When condensation sink remains low then also achieved yield is low.

What comes to goodness of formula 3.12, red lines in figure 4.4 show that yield values are over estimated. That is because of vapor dilution (negligible?? 5e-5) and... other? And fits better to those values with greater seed aerosol mass and condensation sink. Thus chamber wall loss is bigger when aerosol mass (condensation sink) is small. vapor goes to wall in the beginning (of experiment) because it has no other place to go resulting bigger wall loss coefficient  $\gamma$ .

Both black and blue lines fit to data really good and better than red ones. One can see, comparing vapor loss coefficients  $\gamma$  of red and blue fits, that blue one, which

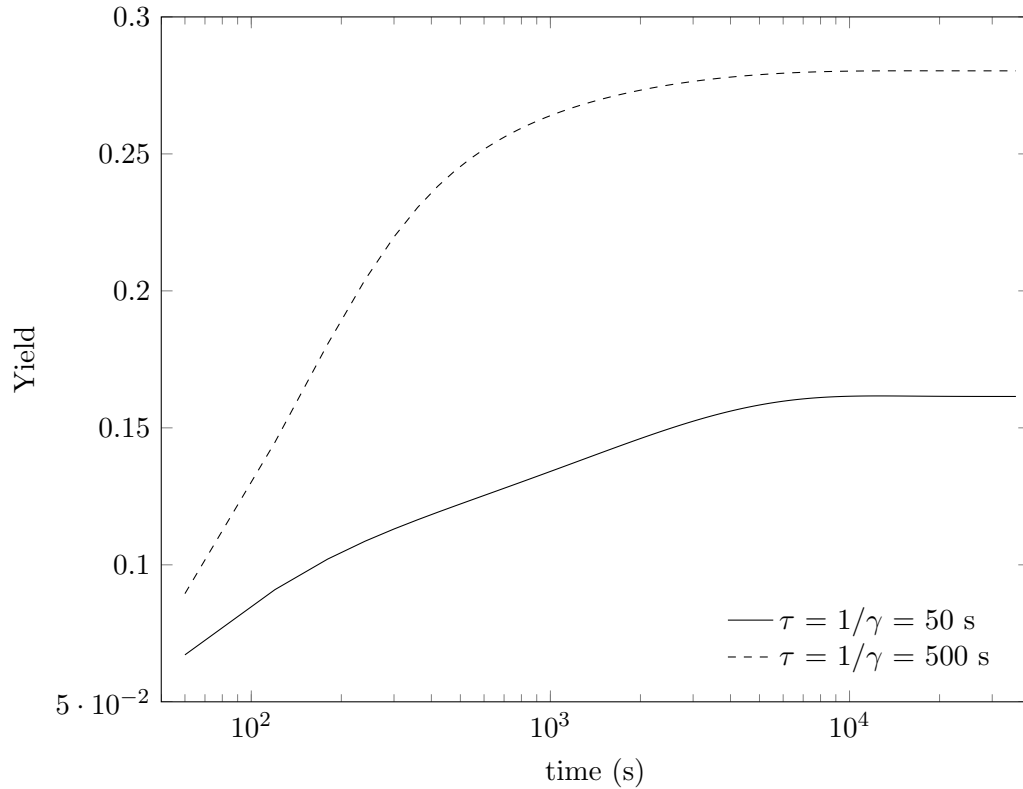


**Figure 4.3:** Aerosol mass yield as function of modelling time for two SLLV lifetimes  $\tau$ . Model initial values were  $D_p = 80$  nm,  $M_{OA} = 5 \mu\text{gm}^{-3}$  and  $P_0 = 50\text{ppb}$ .

agrees better to data, has greater loss coefficient. (Thus this result agrees with earlier conclusion...)

Other reason, why red line fits better to data points with bigger mass, is that it is assumed that condensation sink stays roughly constant during aerosol mass growth (see supplementary). Really CS isn't constant but increases during aerosol growth resulting to bigger values for wall loss coefficient  $\gamma$ .

Increase of CS is relatively bigger for small seeds than for bigger seeds as one can see from figure 4.1. Thus this assumption (red line) is better for bigger aerosol seeds when CS doesn't change so much.

One can get rough values for  $\alpha$  and  $\gamma$  fitting formula 3.12 to CS data...

If also Vtot figure then  $\alpha$  and  $\gamma$  values from distribution data (if density known and spherical particles). If Mtot known then you get

Problem still  $N^{0.37}$

But how mentel or odum or shilling got Yield pictures as function of aerosol mass without problem but we have?

Questions in calculation

CS calc with H2S04 values (CS general function) diff coeff and molemass

Mass calc with H2SO4 molemass, density

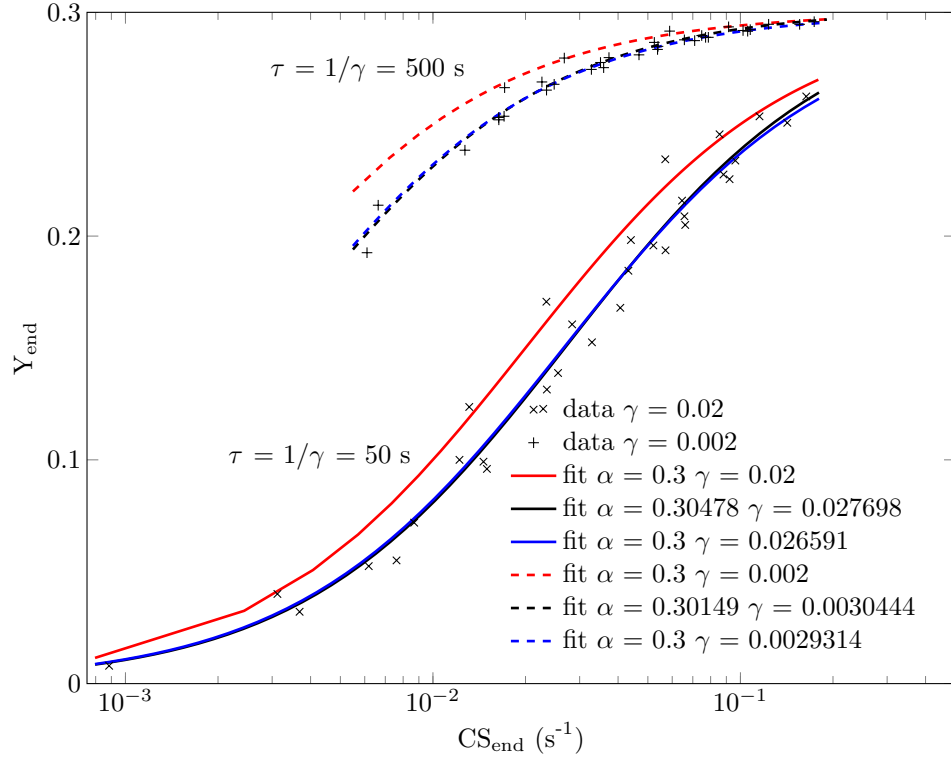


**Figure 4.4:** Presented data points are yield values as function of condensation sink for two different SLLV product lifetimes  $\tau$  used in modelling. Lifetime is inverse of chamber loss rate  $\gamma$ . Data points are fitted to  $\alpha/(1+\gamma/CS)$  with three different ways. Red lines are fitted with constant values for  $\alpha$  and  $\gamma$  which are the same used in model. Black and blue lines are fitted to data using least square method with two parameters  $\alpha$  and  $\gamma$  (black) or one parameter  $\gamma$  and constant  $\alpha$  (blue). Used fitting parameters are shown in legend.

Model run with H<sub>2</sub>SO<sub>4</sub>

Diff coeff in model and CS calculation is for H<sub>2</sub>SO<sub>4</sub>...

Should we change those closer to condensating vapor values?



## 4.2 Results using $C_{10}H_{16}O_{10}$ values

Changed  $D$ ,  $\lambda$ , molar mass of monoterpene precursor  $M_{MT}$  and condensing vapor  $M_{vap}$ , density of particles  $\rho$

To get an idea how condensation sink and secondary organic aerosol mass varies throughout modelling time, in figures 4.5 and 4.6 are presented four examples of condensation sink and aerosol mass with different initial conditions in batch chamber model. All other condensation sinks and aerosol masses of 60 cases are between or near of those lines in figures 4.5 and 4.6.

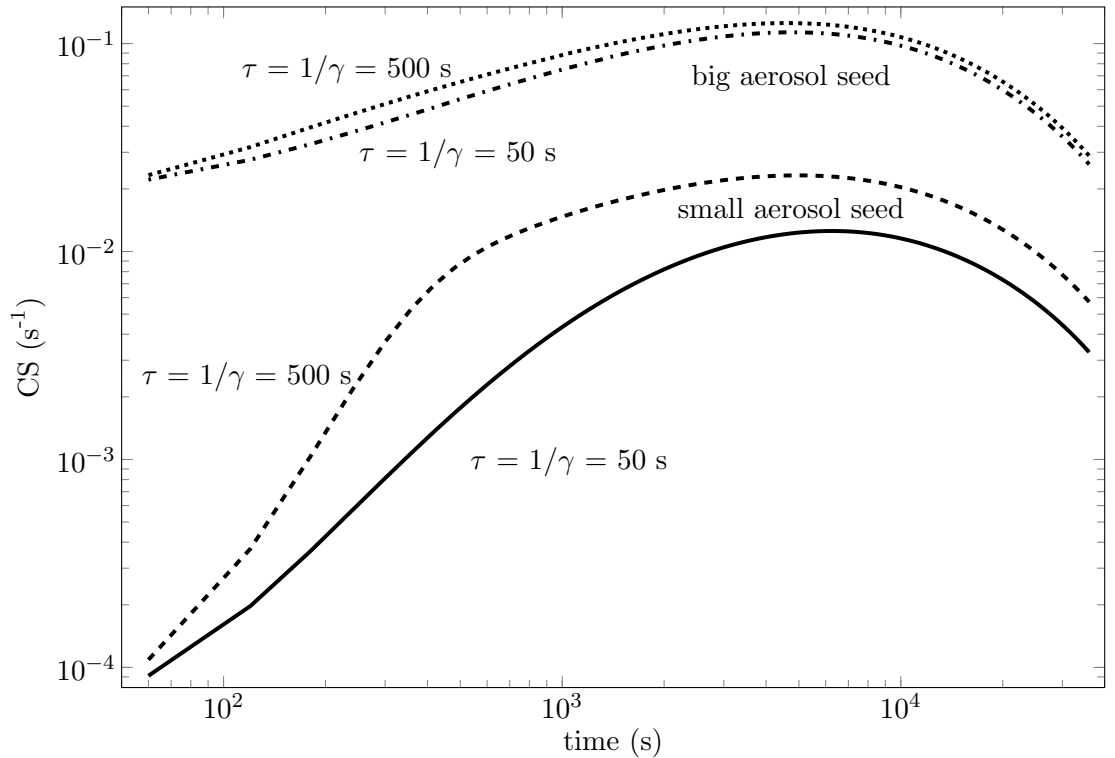


**Figure 4.5:** Condensation sink as function of modelling time in four different cases. Two lines for small ( $D_p = 10$  nm,  $M_{OA} = 3$  ngm $^{-3}$ ) and two lines for big ( $D_p = 80$  nm,  $M_{OA} = 10$   $\mu$ gm $^{-3}$ ) secondary organic aerosol mass seeds are presented with two different SLLV product lifetimes  $\tau$ .

Both condensation sink and aerosol mass grow until dilution loss is bigger than gain from aerosol growth. That happens near  $10^4$  seconds which is about 3 hours and near the times when also aerosol mass yield values are stabilized, see figure 4.7.

In figure 4.8 are aerosol mass yield values, at time when they have reached constant values, as function of aerosol volume. Times needed to stabilise yields are in this modelling from two to three hours, see figure 4.7. That time is considered as end time  $t_{end}$ .

From figure 4.8 can be seen that it not possible to fit all data points to same curve/graph. Yield values increase as aerosol mass seed increases and data points fit

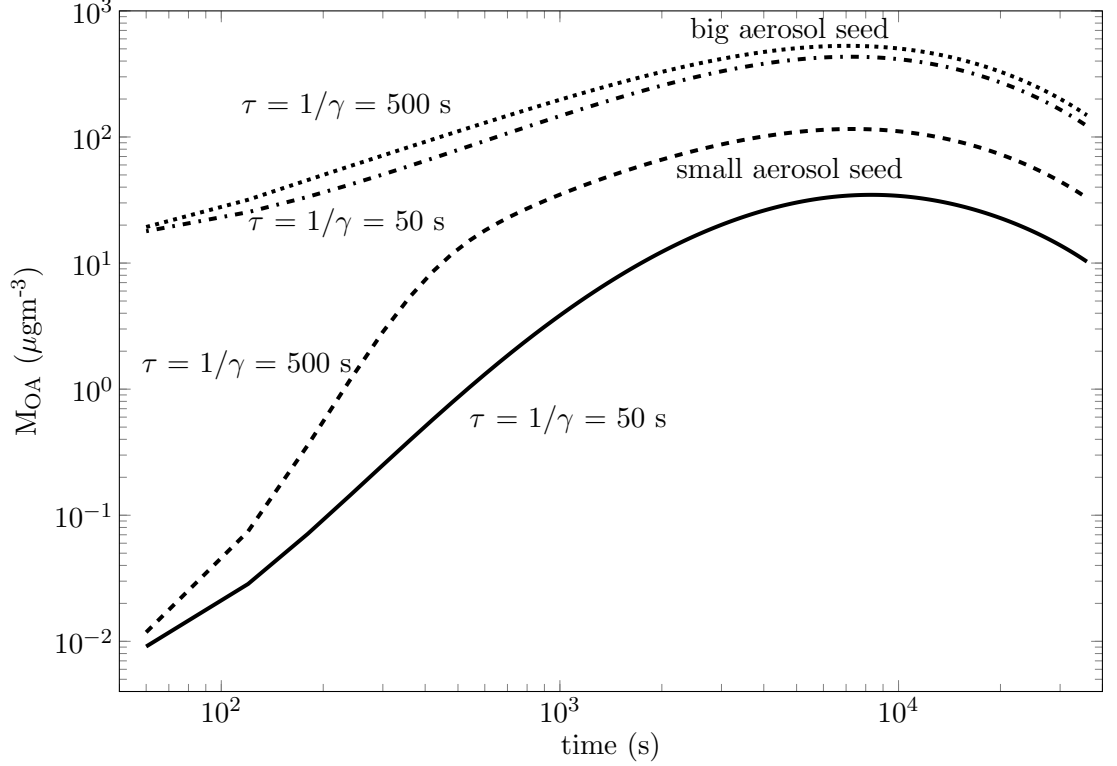


**Figure 4.6:** Secondary organic aerosol mass as function of modelling time in four different cases. Two lines for small ( $D_p = 10$  nm,  $M_{OA} = 3$  ngm $^{-3}$ ) and two lines for big ( $D_p = 80$  nm,  $M_{OA} = 10$  μgm $^{-3}$ ) secondary organic aerosol mass seeds are presented with two different SLLV product lifetimes  $\tau$ .

to different graphs (see red arrow). One can see same effect for both chamber loss rate  $\gamma$  values (blue and black lines). Those points with particle size 10 nm behave similarly because they have pretty much same particle number  $N$  as 80 nm data points.

**Table 4.1:** Used final particle number values  $N_{end}$  in fitting figure 4.8. Values are averages of four data points with nearly equal number concentrations presented in different graphs in figure 4.8.

$M_0$ (μg/cm $^3$ )	$N_{end}$ (1/cm $^3$ )
1	~1900
5	~9000
10	~17000
30	~44000

That's the reason why we propose that yield values should be presented as a function of condensation sink instead of aerosol mass or volume. All data points fit better to one graph as seen in figure 4.9.

One can see, comparing data points with different SLLV lifetimes in figure 4.9, that aerosol mass yields are lower when lifetime is shorter. With short vapor lifetime,

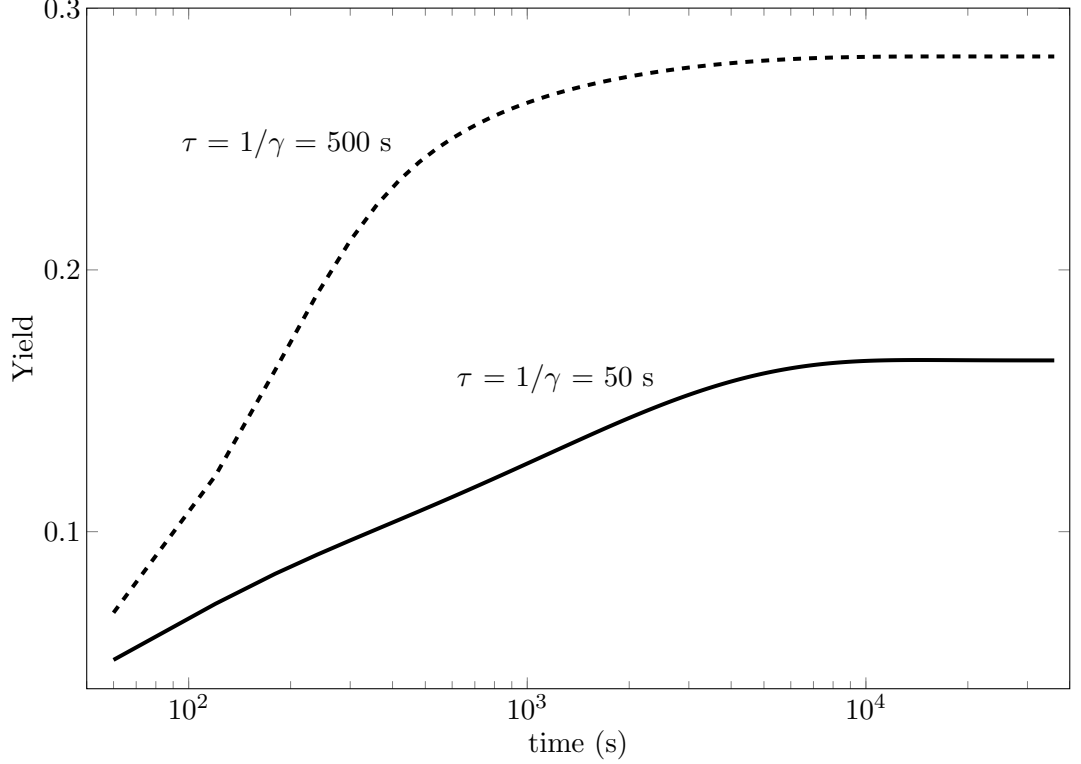


**Figure 4.7:** Aerosol mass yield as function of modelling time for two SLLV lifetimes  $\tau$ . Model initial values were  $D_p = 80$  nm,  $M_{OA} = 5 \mu\text{gm}^{-3}$  and  $P_0 = 50$  ppb.

there is not enough time for aerosol to grow bigger sizes (bigger CS). This happens mainly in chamber studies but shifting to atmosphere, where vapor lifetime is assumed to be much longer, it results bigger yield values. This transfer is presented with black arrows in figure 4.9.

What comes to goodness of formula 3.12, red lines in figure 4.9 show that yield values are overestimated. And fits better to those values with greater seed aerosol mass and condensation sink. Thus chamber wall loss is bigger when aerosol mass (condensation sink) is small. Vapor goes to wall in the beginning of experiment because it has no other place to go, resulting bigger wall loss coefficient  $\gamma$ .

Both black and blue lines fit to data really good and better than red ones. One can see, comparing vapor loss coefficients  $\gamma$  of red and blue fits, that blue one, which agrees better to data, has greater loss coefficient. This result agrees with earlier conclusion.

Other reason, why red line fits better to data points with bigger mass, is that it is assumed that condensation sink stays roughly constant during aerosol mass growth (see supplementary). Really CS isn't constant but increases during aerosol growth resulting to bigger values for wall loss coefficient  $\gamma$  when CS is small.

Third reason is that increase of CS is relatively bigger for small seeds than for bigger seeds as one can see from figure 4.5. Thus this assumption (red line) is better

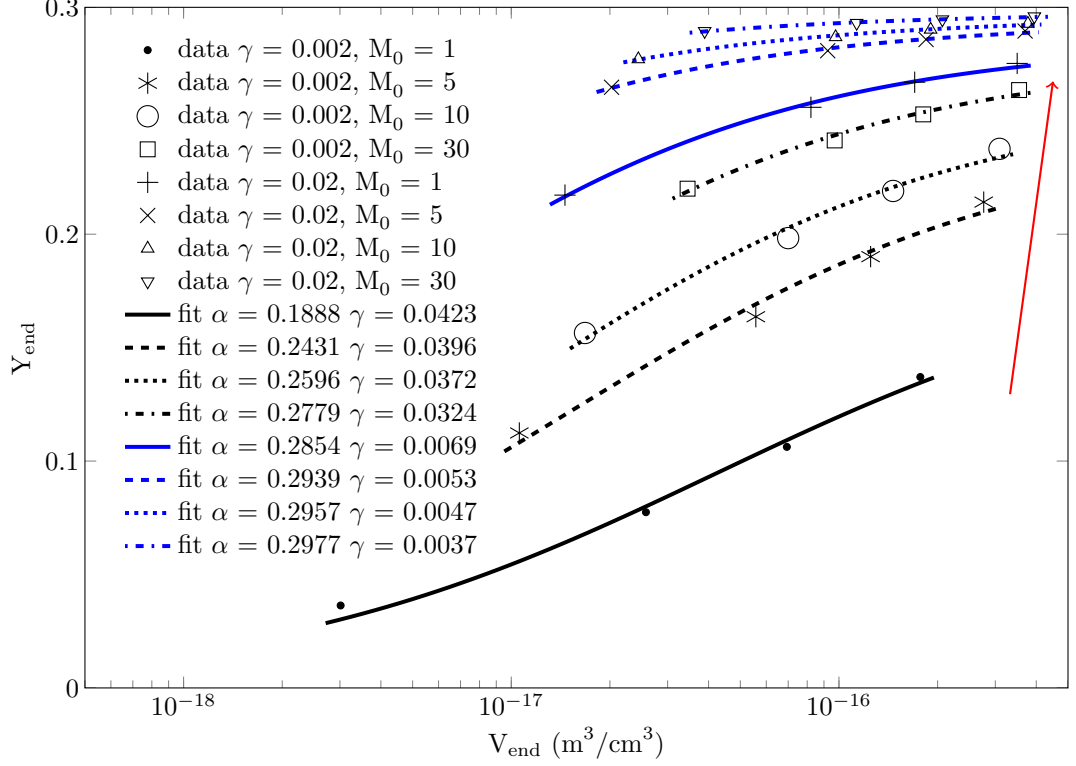


**Figure 4.8:** Presented data points are yield values as function of aerosol particles total volume  $V_{\text{tot}}$  for 80 nm particles with four different mass seeds  $M_0$  ( $\mu\text{g}/\text{cm}^3$ ) and two different SLLV product lifetimes  $\tau$  used in modelling. Lifetime is inverse of chamber loss rate  $\gamma$  ( $\text{s}^{-1}$ ). Data points are fitted to  $\alpha/(1+\gamma/(2 \cdot 10^{-4} \cdot N_{\text{end}}^{0.37} M_{\text{end}}^{0.63}))$ , where  $M_{\text{end}} = \rho V_{\text{end}}$ . Lines are fitted to data using least square method with two parameters  $\alpha$  and  $\gamma$ . Parameter values are shown in legend and used  $N_{\text{end}}$  values in table 4.1. Red arrow represents growth of mass seed  $M_0$ .

for bigger aerosol seeds when CS doesn't change so much.

One can get rough values for  $\alpha$  and  $\gamma$  fitting formula 3.12 to CS data.

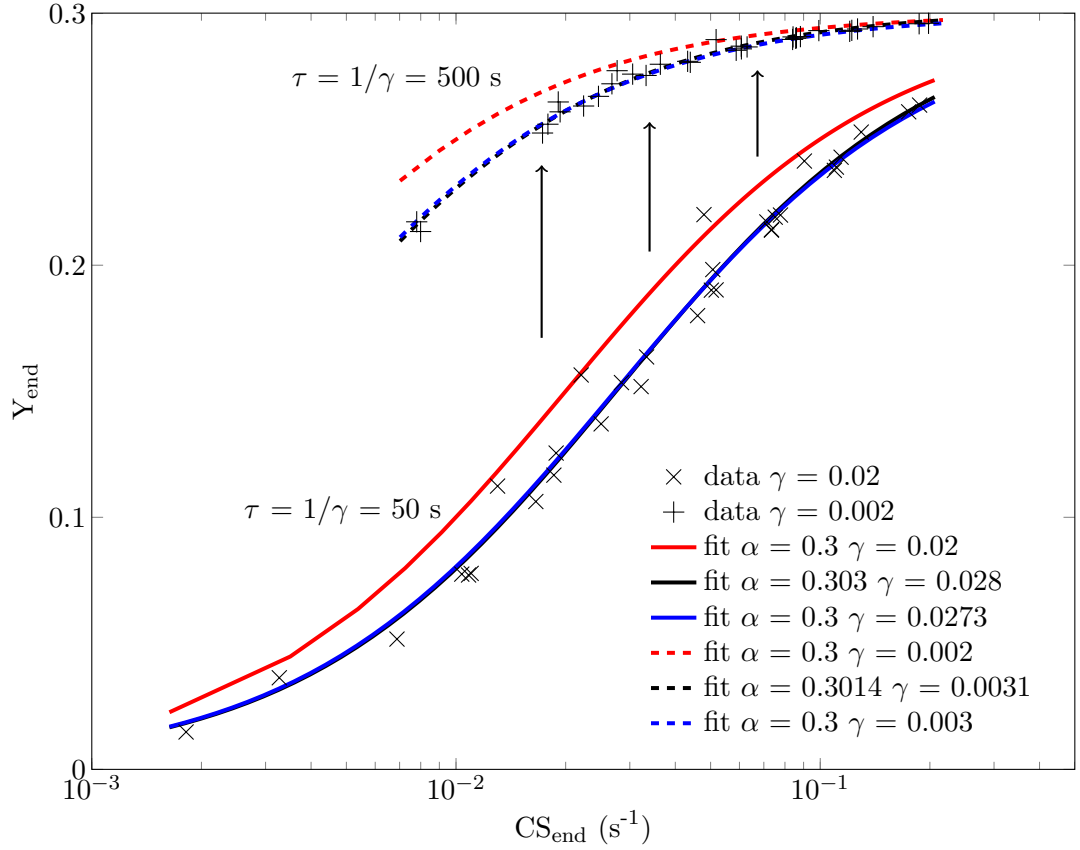


**Figure 4.9:** Presented data points are yield values as function of condensation sink for two different SLLV product lifetimes  $\tau$  used in modelling. Lifetime is inverse of chamber loss rate  $\gamma$ . Data points are fitted to  $\alpha/(1+\gamma/CS)$  with three different ways. Red lines are fitted with constant values for  $\alpha$  and  $\gamma$  which are the same used in model. Black and blue lines are fitted to data using least square method with two parameters  $\alpha$  and  $\gamma$  (black) or one parameter  $\gamma$  and constant  $\alpha$  (blue). Used fitting parameters are shown in legend. Black arrows represents what happens when vapor lifetime grows.

### 4.2.1 Mass- $\alpha$ figures

In this section yields are calculated using precursor molar mass  $M_{MT} = 137$  g/mol to calculate lost precursor mass. In previous section it was 300 g/mol.

From figures 4.10 and 4.11 can be seen that mass yields are higher than molecular/stoichiometric yields (figures 4.8 and 4.9). If stoichiometric coefficient  $\alpha$  of equation 2.24 is wanted, one should use molecular yield. Although mass yields are those which are measured. From stoichiometric  $\alpha_{st}$  to mass  $\alpha_{mass}$

$$\alpha_{mass} = \alpha_{st} \cdot \frac{M_{vap}}{M_{MT}} = 0.3 \cdot \frac{300}{137} = 0.657. \quad (4.1)$$

In conclusion stoichiometric coefficients are not straight seen from mass yields but from stoichiometric yields.

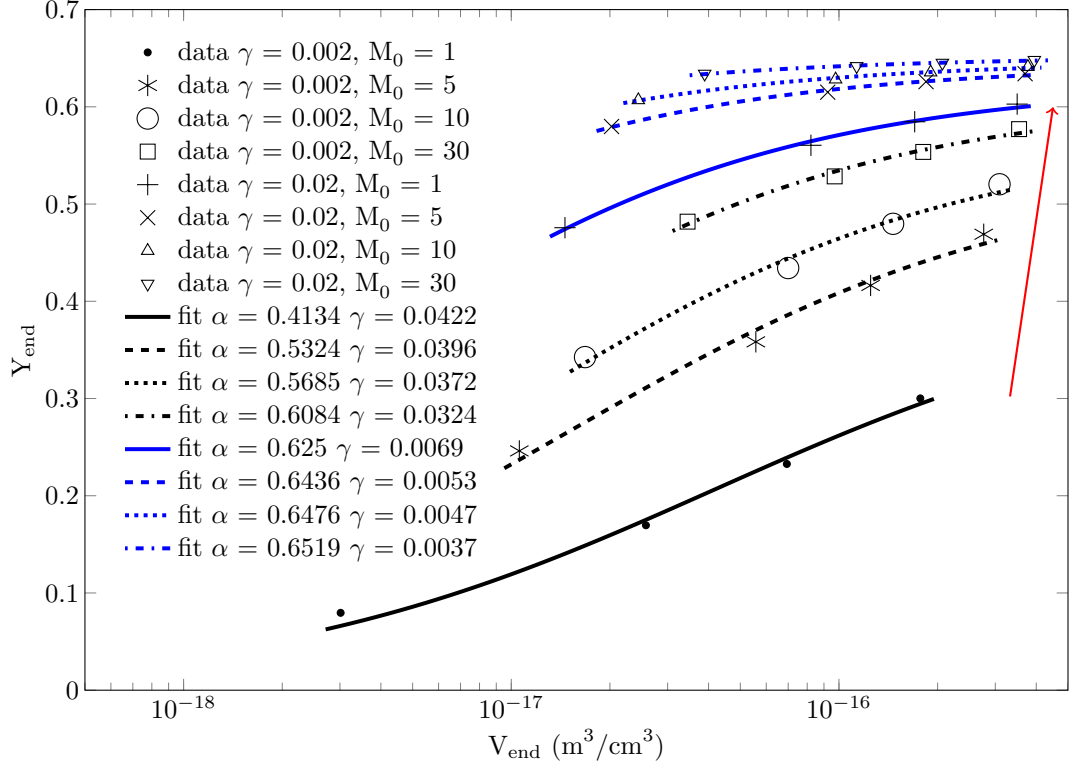


**Figure 4.10:** Presented data points are yield values as function of aerosol particles total volume  $V_{tot}$  for 80 nm particles with four different mass seeds  $M_0$  ( $\mu\text{g}/\text{cm}^3$ ) and two different SLLV product lifetimes  $\tau$  used in modelling. Lifetime is inverse of chamber loss rate  $\gamma$  ( $\text{s}^{-1}$ ). Data points are fitted to  $\alpha/(1+\gamma/(2 \cdot 10^{-4} \cdot N_{end}^{0.37} M_{end}^{0.63}))$ , where  $M_{end} = \rho V_{end}$ . Lines are fitted to data using least square method with two parameters  $\alpha$  and  $\gamma$ . Parameter values are shown in legend and used  $N_{end}$  values in table 4.1. Red arrow represents growth of mass seed  $M_0$ .

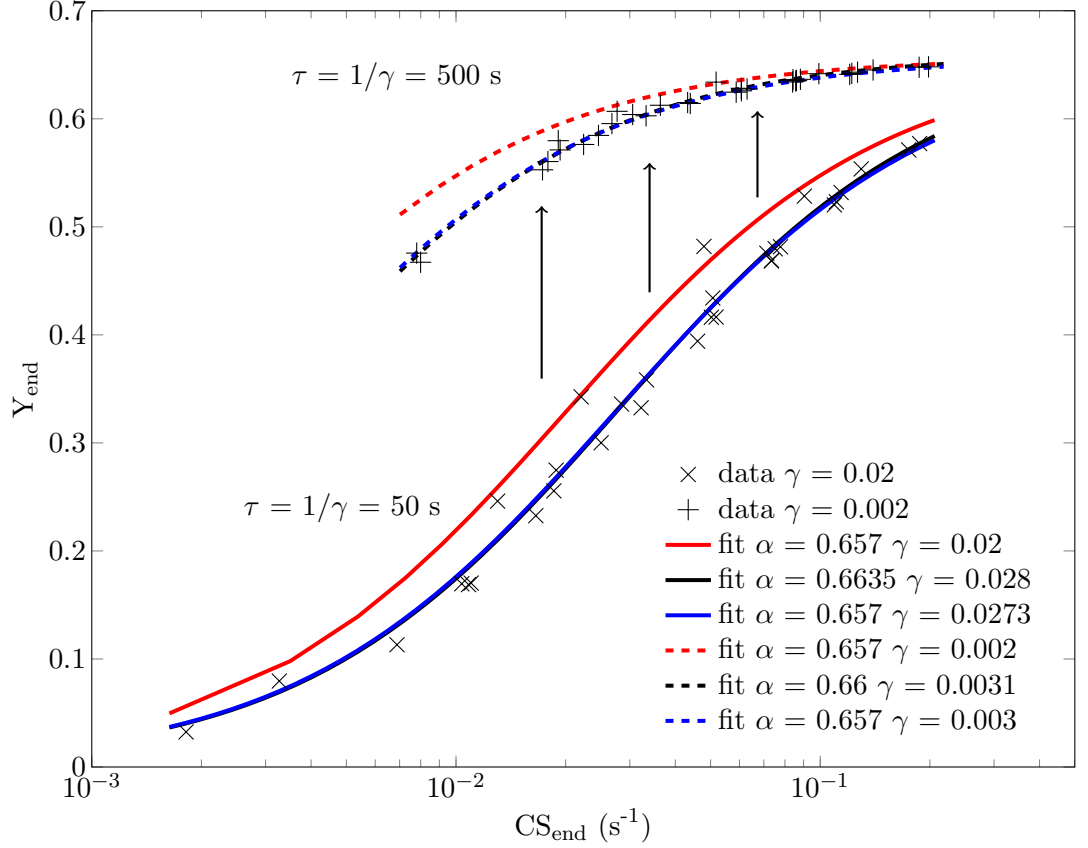


**Figure 4.11:** Presented data points are yield values as function of condensation sink for two different SLLV product lifetimes  $\tau$  used in modelling. Lifetime is inverse of chamber loss rate  $\gamma$ . Data points are fitted to  $\alpha/(1 + \gamma/CS)$  with three different ways. Red lines are fitted with constant values for mass- $\alpha$  and  $\gamma$  which are the same used in model. Black and blue lines are fitted to data using least square method with two parameters mass- $\alpha$  and  $\gamma$  (black) or one parameter  $\gamma$  and constant mass- $\alpha$  (blue). Used fitting parameters are shown in legend. Black arrows represents what happens when vapor lifetime grows.

## 5. MATLAB SCRIPTS AND DATA FILES

Datafiles are located in GitHub path:

For 10 nm particles

\GitHub\AECHAMO\Results and scripts\_mp\SOA formation\Batch  
 \Fixed\_diff\_molemass\10nm\fixed correct lambda\fixed correct density  
 \run\_20130726T203251

And for 80 nm particles

\GitHub\AECHAMO\Results and scripts\_mp\SOA formation\Batch  
 \Fixed\_diff\_molemass\80nm\fixed correct lambda\fixed correct density  
 \run\_20130726T200039

Calculations was done with script:

\GitHub\AECHAMO\calculate and plot\SOA\_calculation\_Yend\_CSend.m

Also all used functions are found in this folder or AEROTOOLS\development repository.

This documentation pdf latex origin:

\GitHub\AECHAMO\documentation\_mp\chamber

Diffusion coefficient variation figure 2.1 made with: \GitHub\AECHAMO\calculate and plot



## 6. CONCLUSION

### 6.1 What next?

DONE-Writing down methods (and theory):

DONE-How model works? Aerosol processes, equations, used coefficients

DONE-How calculations are done? What are calculated from  $dN/dD_p$ ?

How one gets  $\alpha$  and  $\gamma$  from  $dN/dD_p$ ?

DONE-Ask Jyrki for diffusion coefficient, find out D

DONE-Draw pictures  $Y_{end}(V_{tot})$  and fits

DONE- $C_{10}H_{16}O_{10}$  pictures with right values

DONE-yield pictures with precursor P molar mass  $M = 137$  g/mol  $\rightarrow \alpha$  to 0.657

DONE-explain difference between mass yield and molecular yield

DONE-used  $N_{end}$  values

DONE-uniform terminology

DONE- Diff. figure

DONE- references

## REFERENCES

- Dal Maso, M., Kulmala, M., Lehtinen, K. E. J., Mäkelä, J. M., Aalto, P., and O'Dowd, C. D. (2002). Condensation and coagulation sinks and formation of nucleation mode particles in coastal and boreal forest boundary layers. *Journal of Geophysical Research D: Atmospheres*, 107(19):1–10.
- Dormand, J. R. and Prince, P. J. (1980). A family of embedded Runge-Kutta formulae. *Journal of Computational and Applied Mathematics*, 6:19–26.
- Korhonen, H. (2004). Model studies on the size distribution dynamics of atmospheric aerosols. *Doctoral thesis. University of Helsinki*.
- Pirjola, L. and Kulmala, M. (1998). Modelling the formation of  $\text{H}_2\text{SO}_4\text{-H}_2\text{O}$  particles in rural, urban and marine conditions. *Atmospheric Research*, 46(3-4):321–347.
- Reid, R., Prausnitz, J., and Poling, B. (1987). *The properties of gases and liquids*. McGraw Hill Book Co., New York.
- Seinfeld, J. H. and Pandis, S. N. (1998). *Atmospheric Chemistry and Physics - From Air Pollution to Climate Change*. John Wiley & Sons, New York.